

A graphene-based electro-thermochromic textile display

Xiaoqian Ji^{a,b}, Wenwen Liu^a, Yunjie Yin^a, Chaoxia Wang^{a*}, Felice Torrisi^{b,c*}

Received 00th January 20xx,

Accepted 00th January 20xx

DOI: 10.1039/x0xx00000x

Electronic textiles (e-textiles) are rapidly emerging as key enablers for wearable electronics. Graphene and 2D materials have played a major role in enabling truly wearable e-textiles. We demonstrate a textile-based display by using the Joule's heating of a screen printed few layers graphene ink to drive the colour switching of thermochromic polyurethane on cotton fabric. The average temperature of the few layers graphene ink on fabric was voltage-controlled reaching about 43 °C in 45 s at a bias of 12 V and a recovery of < 20 s, with negligible degradation after several heating/cooling cycles. This is used to demonstrate several electro-thermochromic textile displays, representing a breakthrough in e-textiles technology.

Introduction

Wearable electronics is an emerging field, which offers huge potential in healthcare and wellbeing, Internet of Things (IoT) and biosensing applications^{1–3}. Electronic textiles (E-textiles) are a very promising technology, which promises to revolutionize wearable electronics offering breathability, conformability and comfort to wear⁴. Despite all-textile individual electronic components⁵ and integrated circuits have been demonstrated⁶, only few reports have attempted to achieve textile-based displays⁷. Thermochromic textile devices have already been demonstrated using metal oxide (such as CoO and Pb₃O₄), leuco dye or polymer (such as polydyne) through various methods of textile integration, such as coating⁸, spinning⁹, and dyeing.¹⁰ Thermochromic dyes are composed of thermochromic molecules (TMs). These molecules have the property to change colour when exposed to an increase of the surrounding

temperature (above a certain critical temperature, T_c). The change in colour is caused by the variation of the structural conformation of the molecule, induced by the thermal energy¹⁰. Thermochromic dyes have attracted much attention in medicine¹¹, wearable devices¹² and security materials because of its application as storage element in memories¹³, temperature switches¹⁴, colour changing paints¹⁵ and anti-counterfeiting devices^{15,16}. The leuco dye is one of the most common thermochromic dyes consisting of a colour former (i.e. conjugated molecule, which is responsible for the colour combination) and a developer (typically weak acids such as bisphenol A, gallates, hydroxybenzoates and hydroxycoumarin derivatives) in a nonvolatile organic solvent (such as methyl stearate)^{17–19}. The weight ratios of the colour former, the colour developer and the solvent is key in engineering the thermochromic dye. If the solvent is too much, the thermochromic dye will be too light or even colourless below T_c . On the contrary, if the solvent is too little, the thermochromic dye will change colour when above T_c . However, the presence of bisphenol A in leuco dyes, generates major environmental concerns and the solvent leakage upon heating²⁰ (when the leuco dye reach thermochromic temperature, the solvent is changed to liquid from solid¹⁸) make leuco dyes unsuitable for textile applications²¹. Stimuli-responsive functional materials have been investigated as a suitable alternative. Ref²² combined red-green-blue (RGB) thermochromic materials (such as DEBN, cyan-6, yellow-1, and blue-220) and luminescent materials (such as Eu(III)(TTA)₃phen and Alq₃) to obtain thermoresponsive dual-mode (define as red-green-blue colouration and fluorescence) representations in RGB colours with large contrast (from RGB to white). A polyurethane-based fluorescent dye was synthesized by attaching a fluorescent dye (such as 4-amino-N-cyclohexyl-1,8-naphthalimide) to polyurethane chains by capping reaction (through a reaction of –NH₂ and –NCO) resulting in a fluorescence intensity increase with above T_c ²³. The thermochromic polyurethane is mainly prepared by mixing pure polyurethane with thermochromic dyes. A waterborne UV-curable polyurethane acrylate/SiO₂

^a Key Laboratory of Eco-Textile, Ministry of Education, College of Textile Science and Engineering, Jiangnan University, Wuxi, 214122, China. Email: wangchaoxia@sohu.com

^b Cambridge Graphene Centre, Department of Engineering, University of Cambridge, 9 JJ Thomson Avenue, Cambridge CB3 0FA, UK. Email: ft242@cam.ac.uk

^c Molecular Sciences Research Hub, Department of Chemistry, Imperial College London, 80 Wood Lane, London W12 0BZ, UK. Email: f.torrisi@imperial.ac.uk

† Electronic Supplementary Information (ESI) available. See DOI: 10.1039/x0xx00000x

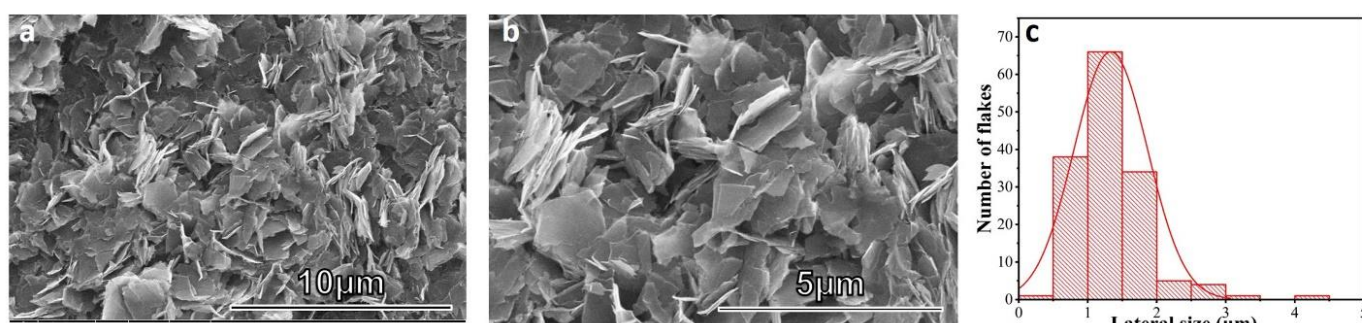


Fig. 1 (a) and (b) SEM images of GNP flakes; (c) Histogram of the lateral flake size for the GNP ink after 70 cycles of microfluidic exfoliation.

nanocomposites incorporating nanosilica was prepared using a new form of sol-gel method and mixed with inorganic thermochromic dyes to make a polyurethane-based thermochromic ink⁸. Recently ref²⁴ demonstrated a thermochromic textile based on UV-induction polyurethane coating mixed with Rhodamine thermochromic dye. The textile showed thermochromic behavior at ~ 50 °C under magnetic heating with UV induction.

Electrically-driven thermochromic switching was also proposed by ref²⁵. The device was achieved by weaving metallic yarns within the fabrics and then paint thermochromic inks on top them. Ref²⁶ deposited a thermochromic ink on one side of a textile substrate and use metal wires as heating elements on the other side, achieving a temperature, $T \sim 50$ °C at a voltage bias (V_{bias}) of 7 V. Ref²⁷ also prepared an electro-thermochromic paper with a commercial leuco dye as the thermochromic ink, which achieved switching at $T \sim 45$ °C at $V_{\text{bias}} \sim 4$ V.

However, this strategy has its own drawbacks since the colour change can only happen in the region close to the conductive yarn when a current passes through it. Recently, the combination of electric heaters from conductive coatings and colour-changing dyes from TMs has been exploited to demonstrate an electro-thermochromic textile. This process allows coating or printing of specific pattern enabling electro-thermochromic image and text. For example, ref.²⁸ described the production of conductive non-woven mats of poly-3,4-ethylenedioxythiophene (PEDOT) using electrospinning. In this case, when an electric current passes through the PEDOT film producing sufficient heat ($T \sim 100$ °C at $V_{\text{bias}} \sim 10$ V), the coated thermochromic ink undergoes a colour change. Recently, electromagnetic interference shielding fabric, and stable Joule heating response based on CNTs network-embedded poly (vinyl alcohol) (PVA) composite film were also reported.²⁹⁻³¹ More recently, ref. 32 prepared a coaxial multilayer monofilament whose conductive core layer could trigger the colour change of the external thermochromic layer upon resistive heating. However, the conductivity of the monofilament is low (1×10^{-2} S/cm), requiring a high voltage to induce a thermochromic colour change, becoming unsuitable for wearable applications. Graphene and graphene nano-platelets (GNPs) also have been the focus of intense research as suitable materials for electric heating³³, as well as biocompatible^{34,35} and wearable electronics^{6,36,37}.

Following on from previous works on UV-induced thermochromic textile²⁴ using Rhodamine B ethylenediamine

derivative molecules, here we demonstrated a screen-printed electro-thermochromic textile (ET) on cotton fabric, consisting of a UV-induced thermochromic polyurethane layer based on Rhodamine B ethylenediamine derivative molecules and GNP electrodes. The electro-thermochromic switching of the fabric from magenta to white was controlled via Joule's heating from an applied voltage, reaching $T \sim 43$ °C at $V_{\text{bias}} \sim 12$ V within 45 s and a recovery of < 20 s. We then used this technology to demonstrate an electro-thermochromic textile display (ETD).

Results and discussion

The voltage-controlled heating of the screen printable GNP ink is key to enable the electro-thermochromic devices on textile. Here we first fabricate the electrically and thermally conducting fabric by screen printing the GNP ink on cotton fabric and then investigate the surface morphology, the electrical properties of the printed GNP ink, and the performance as a heater GNP-coated fabric.

Graphene nano platelets ink

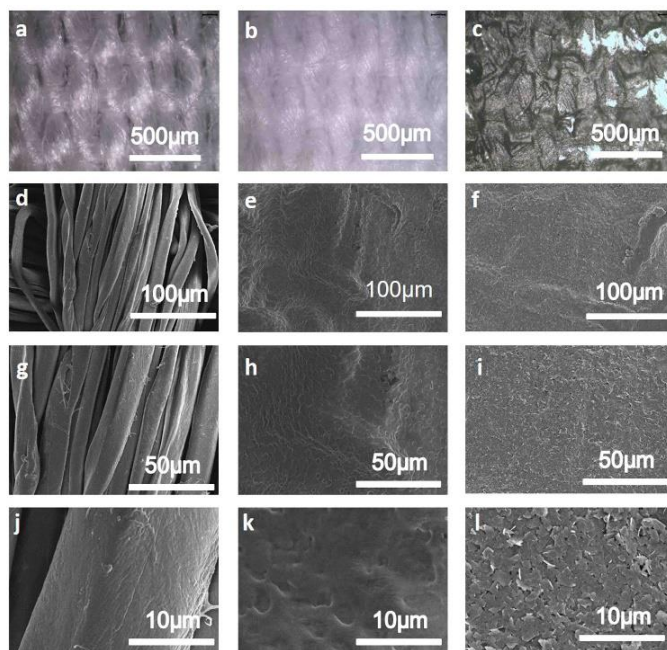


Fig. 2 Optical microscope images of: (a) control cotton fabric, (b) PU-treated cotton fabric, (c) GNP fabric, SEM images of (d, g, j) control cotton fabric, (e, h, k) PU-treated cotton fabric, (f, i, l) GNP fabric

The GNP ink was prepared via microfluidic exfoliation of graphite (see methods). Scanning electron microscopy (SEM) was used to investigate the surface topography and the lateral size of the graphene flakes. Fig.1 (a) and (b) show SEM micrographs with the typical surface topography of GNP ink. Statistics of the lateral size (defined as the longest dimension) of the GNP flakes (Fig.3 c) reveals that mainly this is peak at 1-1.5 μm .

Graphene nano-platelets fabric (GNP fabric)

The white-coloured control cotton fabric is shown in Fig.2 (a). After polyurethane treatment, the cotton fabric is dried in the oven at 60 $^{\circ}\text{C}$ for 10 min to remove any residual water, resulting in a layer film on the surface of the cotton fabric as the Fig.2 (b). The GNP fabric (shown in Fig.2 c) is prepared by screen printing the GNP ink on polyurethane (PU)-treated cotton fabric forming a GNP ink layer (7.6 μm thick) on the surface. Figs 2 (d-l) show the optical SEM images of the control cotton fabric (Figs 2 d, g, j), PU -treated cotton fabric (Figs 2. e, h, k) and GNP fabric (Figs.2 f, i, l) at different magnifications. The SEM images (Figs.2 d, g, j) show a typically fibrous structure with the fibres twisting with each other, producing a quite rough fabric surface. Comparing Fig. 2 (e) with Fig. 2 (d), the surface of the cotton fabric is evenly covered with a film and the texture of the fabric is faintly seen. The surface of the pre-treated cotton fibre is covered with a layer of polyurethane film. The SEM in Fig. 2 (f) shows how the GNP ink uniformly conforms to the pre-treated cotton fabric. Compared with the control cotton fabric, the C content of the GNP fabric was increased (shown as Figure S1).

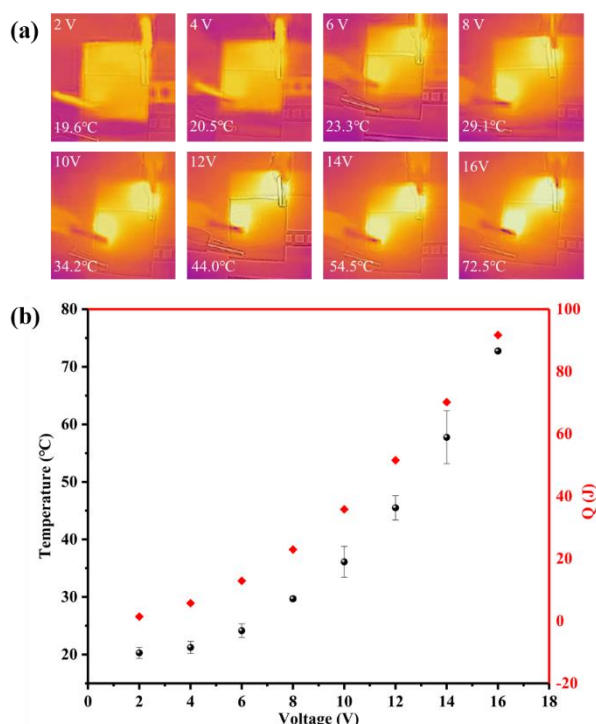


Fig. 3 (a) Infrared thermal images of the conductive fabric at various V_{GNP} ; (b) plot of the temperature versus V_{GNP} .

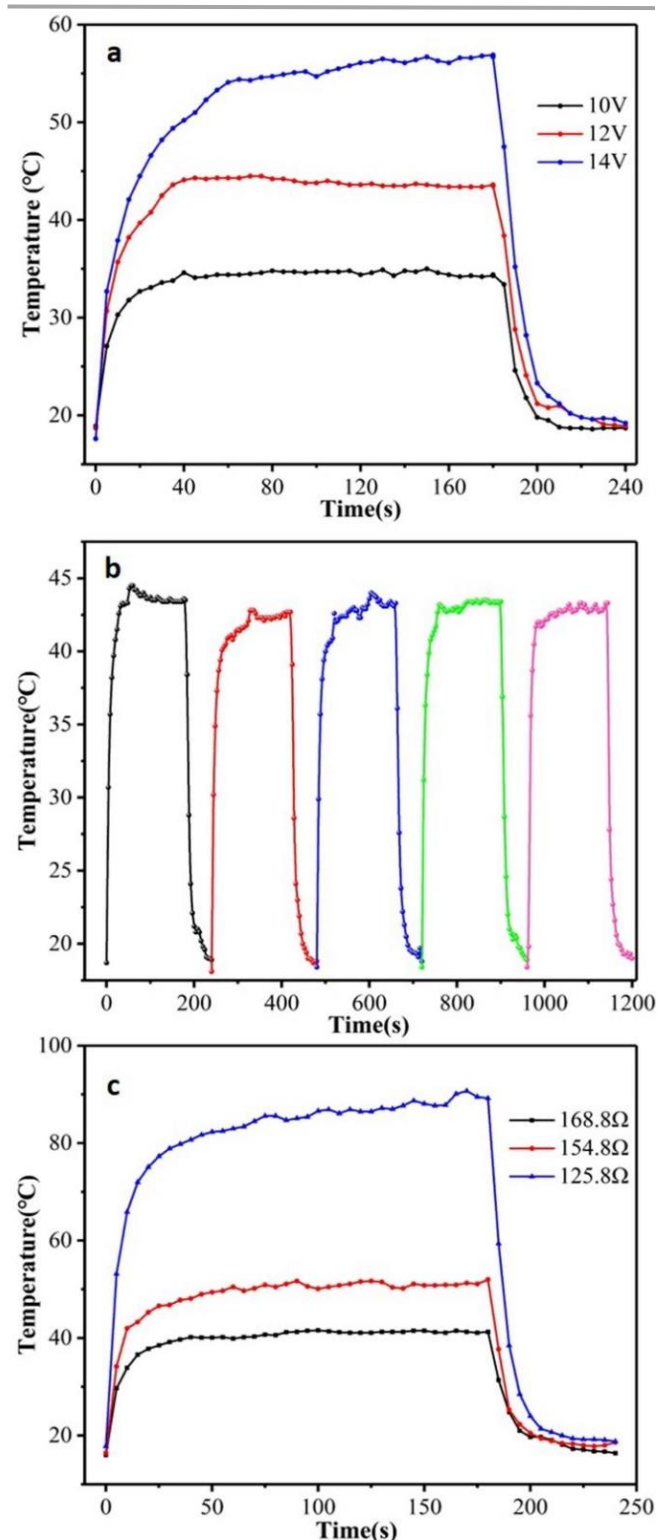


Fig. 4 (a) Temperature profiles of the GNP fabric at different V_{GNP} ; (b) Temperature response of the GNP fabric over 5 cycles at $V_{\text{GNP}} = 12 \text{ V}$, each cycles is 4 min long; (c) Temperature profiles of the GNP fabric operated at different biases;

Electrical and thermal characterization of the GNP fabric

The electrical and heating properties of the GNP fabric are characterized on a 2×2 cm sample revealing a sheet resistance,

$R_s \sim 169 \Omega$ and the conductivity $\sigma \sim 778.6 \text{ S/m}$, which is consistent with the conductivity values reported by previous works³⁵. The heating properties of the GNP fabric are investigated by monitoring the evolution of the temperature by an infrared camera (see methods) as a function of the applied voltage (V_{GNP}) across the GNP fabric (between 2 V and 16 V), Fig. 3. The thermal images show a clear heating of the GNP fabric as a function of V_{GNP} , increasing from $T \sim 19.6 \text{ }^\circ\text{C}$ to $\sim 72.5 \text{ }^\circ\text{C}$.

The heating of our GNP fabric can be described by Joule's law which defines the heat (Q) dissipated from a resistive material when voltage (or current) is applied as follows^{36,37}:

$$Q = V^2/Rt$$

where V is applied voltage, $R = 335 \Omega$ is the resistance of the conductive fabric (see methods) and t is the operating time. The measured temperature change and calculated Q as a function of voltage is shown in Fig. 3 (b). Temperature profiles of the conductive fabric under different biases are measured as shown in S2. At $V_{\text{GNP}} = 6 \text{ V}$, only $\sim 19\%$ increase of temperature was detected on the GNP printed pattern. A change of regime, takes place at higher voltage and the temperature began to rise significantly going from $T \sim 23.3 \text{ }^\circ\text{C}$ at $V_{\text{GNP}} = 6 \text{ V}$ to $T \sim 72.5 \text{ }^\circ\text{C}$ at $V_{\text{GNP}} = 16 \text{ V}$. This large temperature modulation of the GNP fabric was ascribed to the remarkable electrical conductivity of the GNP ink and the heat dissipation of cotton fibres.

Fig. 4 (a) shows the temperature profiles of the GNP fabric, as a function of the t for $V_{\text{GNP}} = 10 \text{ V}$, 12 V and 14 V . All curves show a similar trend with a time response (τ , defined as the time required to reach the steady-state temperature which was above 90% of highest temperature from room temperature) of $\tau = 45 \text{ s}$, $\tau = 45 \text{ s}$ and $\tau = 60 \text{ s}$ for $V_{\text{GNP}} = 10 \text{ V}$, 12 V and 14 V respectively. In this case, when $V_{\text{GNP}} = 10 \text{ V}$, only about $T \sim 15 \text{ }^\circ\text{C}$ increase was observed reaching about $35 \text{ }^\circ\text{C}$ after $\tau = 40 \text{ s}$. At $V_{\text{GNP}} = 14 \text{ V}$, the GNP fabric reached $\sim 60 \text{ }^\circ\text{C}$ after $\tau = 60 \text{ s}$. The steady-state temperatures were reached for all samples in less than 60 s, demonstrating a faster response^{41,42} than graphene-based electro-thermal films which reaches $T \sim 42 \text{ }^\circ\text{C}$ when 60 V is applied for 2 min⁴³. In all our GNP fabrics, the temperature

remained stable upon constant voltage applied and then returned to room temperature ($T \sim 20 \text{ }^\circ\text{C}$) after about 60 s when power was off. This cooling rate can be explained by the nature of the cotton fabric that allows the heat to be very effectively dissipated by the material (the thermal conductivity of cotton fabric is $0.026\text{--}0.065 \text{ W/mK}$ ⁴⁴).

To investigate the stability of the GNP fabric, repeated heating and cooling cycles are carried out (as show in Fig. 4 b and Figure S3). The temperature change of the GNP fabric was recorded over a period of 4 min (heating 3 min at $V_{\text{GNP}} = 12 \text{ V}$ and cooling 1 min at $V_{\text{GNP}} = 0 \text{ V}$) for 5 cycles. As showed in Fig. 4 (b), the heating/ cooling curve remained almost unchanged after several cycles, reaching constantly $T \sim 42 \text{ }^\circ\text{C}$ at 12 V for 40s, after several heating and cooling cycles, indicating a good stability and repeatability. During each heating process, the temperature increased from room temperature ($T \sim 20 \text{ }^\circ\text{C}$) to a steady value of $T \sim 43 \text{ }^\circ\text{C}$ in the initial 1 min, revealing a high heating rate of the GNP fabric. In addition, in this case the temperature of the GNP fabric gradually dropped to ambient temperature after 60 s since the voltage was set to $V_{\text{GNP}} = 0 \text{ V}$, thanks to the thermal conductivity of the cotton fabric. The time-dependent temperature profiles of the GNP fabrics with different R_s values is shown in Fig. 4 (c). The temperature change of the GNP fabric was recorded with a period of 4 min (heating 3 min at $V_{\text{GNP}} = 12 \text{ V}$ and cooling 1 min at $V_{\text{GNP}} = 0 \text{ V}$). The value of Q results affected by the resistance of the GNP fabric. At same voltage, the temperature of the GNP fabric is inversely proportional to R_s , thus confirming the heating by Joule effect of the GNP fabric. For $R_s \sim 126 \Omega$, the temperature of the GNP fabric reaches $T \sim 90 \text{ }^\circ\text{C}$, while it only reaches about $40 \text{ }^\circ\text{C}$ for $R_s \sim 169 \Omega$. The conductivity of our GNP fabric is higher than that reported for graphene anodes and cathodes, (e.g. in microbial fuel cells)⁴⁵.

Electro-thermochromic cotton fabric performance

We developed a colour-changing smart fabric and a textile display by combining the colour changing property of the

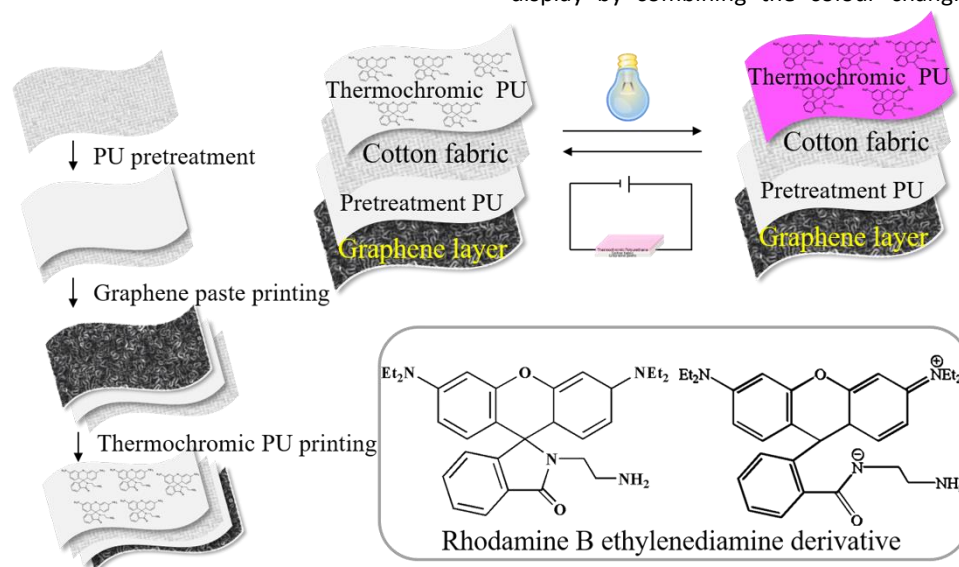


Fig. 5 The schematic diagram of the procedure used to fabricate the ET. In the frame the molecular structure of the two Rhodamine B derivatives.

thermochromic polyurethane ink and the GNP fabric heater as shown in Fig. 5. The Rhodamine B ethylenediamine derivative thermochromic polyurethane ink was screen-printed on one side of the PU-treated cotton fabric, while the GNP ink was screen-printed on the other side (Fig. 5). The choice of depositing the two inks on opposite sides aims to maximize the colour changing property of the thermochromic dye. The layer of polyurethane reduced the surface roughness³⁸ of the fabric and prevented the absorption of the inks into the cotton fabric. The colour-changing property of the ET was investigated by monitoring colour parameter (i.e. K/S, where a^* corresponds to the red and green colour combination and b^* corresponds to yellow and blue colour combination) as a function of V_{GNP} . The darker the red, the larger the a^* . Fig. 6 (a) shows how the colour of the thermochromic coating gradually disappears as the applied voltage increases.

This is the result of the UV induction which modifies the conjugate structure of Rhodamine B ethylenediamine derivative in the chemical composition of the polyurethane ink,

hence resulting in a change of the polyurethane optical properties⁴⁶. Our transparent thermochromic polyurethane starts reflecting in the region around magenta ($\lambda_{\text{max}} = 550\text{nm}$) following the UV induction. It then returns colourless upon heating. The optical images of our ET at different voltages are shown in Fig. 6(a). Firstly, the thermochromic coating on the ET was activated by a treatment irradiation at $\lambda = 254\text{ nm}$ for 3 min. This allows the lactam ring structure of Rhodamine B ethylenediamine derivative moiety in the thermochromic polyurethane to gradually change to an open-loop state with a quinolone structure²⁴. Then we apply an increasing voltage, from $V_{\text{GNP}} = 2\text{ V}$ to $V_{\text{GNP}} = 16\text{ V}$. We can see the ET returning white as the applied voltage increased above $V_{\text{GNP}} = 10\text{ V}$. This is because the Q generated by the GNP ink is sufficient to degrade the quinolone structure in the thermochromic ink, back-converting it to the colourless lactam ring when $V_{\text{GNP}} > 10 - 12\text{ V}$. A $V_{\text{GNP}} = 12\text{ V}$ corresponds to a higher temperature than T_c , which consistently gives a transparent thermochromic coating. In the heating process the GNP coating is the heat source, which transfers heat to the thermochromic polyurethane by radiation and conduction, as shown in the schematic of ET in Fig. 5.

An electro-thermochromic textile display

A series of ETDs are prepared by screen printing the GNP ink, following the steps in Fig. 5 (Figs 6 b, c, d). The thermochromic polyurethane ink was screen printed on the other side of the PU pre-treated cotton fabric with a series of predetermined patterns, "JNU" (Figs 6 b), a horseshoe (Figs 6 c) and a butterfly (Figs 6 d). The thermochromic pattern is then activated by UV induction at $\lambda = 254\text{ nm}$ giving rise to the patterns in magenta. A voltage $V_{\text{GNP}} > 10 - 12\text{ V}$, turns the patterns colourless as shown in Figs 6 b, c, d. Also in this case, we attribute the colour change of the printed pattern to the Joule heat generated by the GNP ink printed at the back of the fabric. Fig 6 (e, f) and Table S1 show the colour parameters (colour difference, ΔE , the K/S value, a^* , b^*) of the ET as a function of λ for a V_{GNP} range between 2 V to 16V. The K/S value shows peaks at 560 nm which are in agreement with the standard peaks for Rhodamine B ethylenediamine derivative. In particular the reference peak at $\lambda = 560\text{ nm}$ decreased as the voltage increased and the a^* was also decreased, which confirms the colour change of the ET and the patterned ETD from magenta to white.

Conclusion

We have obtained electrochromic cotton fabrics and electrochromic textile-based displays using the thermal dissipation of a screen printed graphene-based ink to drive the colour switching of a thermochromic polyurethane ink coated on fabric. The surface of graphene-coated fabric was uniformly covered with graphene sheets, which provided the conductivity of the fabric. The graphene-based fabric generated heat by Joule effect upon voltage bias reached $T \sim 43\text{ }^\circ\text{C}$ at 12 V. When further coated by thermochromic polyurethane and activated by UV induction, the composite fabric switched from magenta

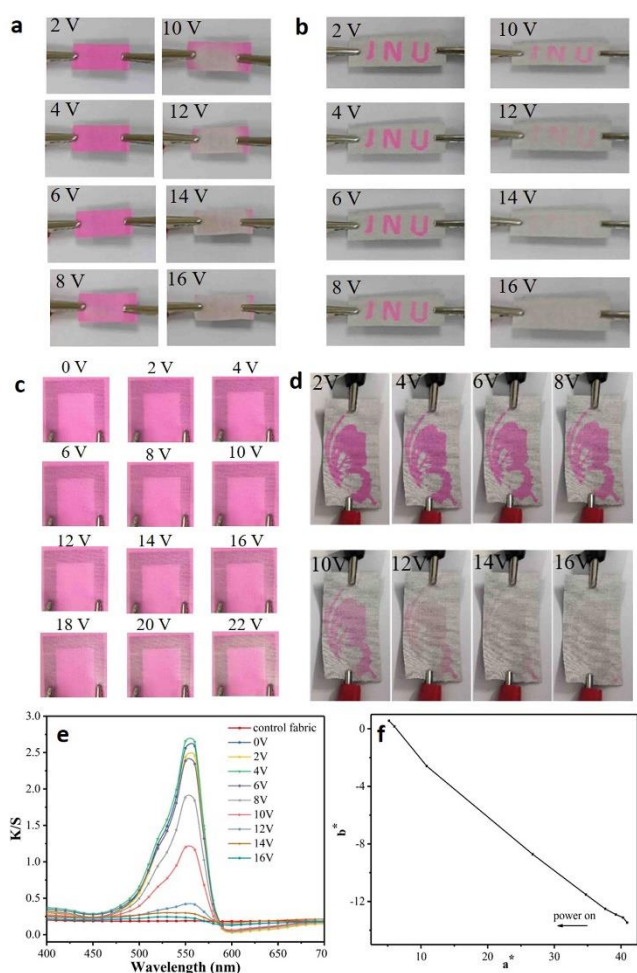


Fig. 6 (a) Photographs of ET (1 cm \times 2 cm) showing smart colour- changing effect as a function of V_{GNP} (b) Photographs of ET (1 cm \times 3 cm) showing smart colour- changing effect as a function of V_{GNP} ; (c) Photographs of ET with a horseshoe pattern, showing smart colour- changing effect as a function of V_{GNP} ; (d) Photographs of ET with butterfly pattern, showing smart colour- changing effect as a function of V_{GNP} ; (e) The K/S curves of the ET as a function of V_{GNP} ; (f) The a^* and b^* of the ET as a function of V_{GNP} .

to white upon applied voltage of 10 V, demonstrating suitable electro-thermochromic switching. The structure of the thermochromic polyurethane was changed to an open-loop state with a quinolone structure and returned to white when the applied voltage increased with the close-loop state of thermochromic polyurethane. This work paves the way for large area, fast and stable thermochromic textile displays in the future.

Methods

Materials

The UV-induced thermochromic polyurethane ink was homemade²⁴. (more details in S2). Timrex KS25 graphite, sodium desoxycholate (SDC) and carboxymethylcellulose sodium (CMC) were supplied by Aldrich chemical. The water-soluble thermal was purchased from Jining Baichuan Chemical Co., Ltd. The printing thickener was supplied by Transfar Co., Ltd.

Formulation of the graphene-based ink

The GNP ink was prepared by dispersing graphite flakes (Timrex KS25) in deionized water (DIW) with Sodium desoxycholate (SDC, 10 mg/mL) followed by a microfluidic exfoliation (M110-P Microfluidizer; Microfluidics)⁶ for 70 cycles obtaining a graphene-based dispersion. Sodium carboxymethyl cellulose (CMC; 7.5 g/L) was blended with the graphene-based dispersion at 60 °C to obtain a GNP ink suitable for screen printing.

Fabrication of the electro-thermochromic cotton fabric and display

The electro-thermochromic cotton fabric ET was prepared by screen printing on a polyurethane coated cotton fabric the graphene heater electrode on the back side of the fabric and the thermochromic UV-induced polyurethane on the front side of the fabric by the following steps:

Cotton fabric pre-treatment

The cotton fabric was pre-treated with water-soluble thermal curing polyurethane (65%), DIW (33%) and thickener (2%). Then the cotton fabric was oven dried at 60 °C for 10 min and 100 °C for 5 min to prepare the pre-treated cotton fabric, denoted as PU pre-treated cotton fabric.

Printing of GNP ink

The GNP ink is deposited via screen printing on the polyurethane-treated cotton fabric followed by a drying step at 60 °C for 10 min. The conductive fabric was denoted as GNP fabric.

Printing of thermochromic polyurethane

The screen printing with UV induction thermochromic polyurethane on the back of conductive fabric. Then the electrothermochromic fabric was dried at 60 °C for 10 min and baked at 130 °C for 5 min.

Electron microscopy characterization

The original graphene ink was dried to prepare the sample for scanning electron microscopy. The surface morphology of conductive fabric was also investigated by SEM. A statistical analysis of over 150 flakes of the original GNP ink were used to estimate the statistics of the lateral size (defined as the longest side of the flake).

Sheet resistance measurements

The sheet resistance of conductive fabric was measured by four-point probe system (KEITHLEY 2400 Source Meter Unit, US). The final resistance value of the fabric was measured with 10 different positions and averaged.

Thickness measurements

The thickness of the GNP flakes was measured with a fabric thickness test equipment (YG141, Changzhou Second Textile Machinery Factory, China).

Thermal and electro-thermochromic measurements

The average temperature of the fabric surface was monitored with an infrared camera (FLIR Ex). The infrared images of the conductive fabric were acquired at various V_{GNP} applied across the GNP, with an exposure time of 2 min. The electrothermochromic behaviour of the GNP fabric was investigated at various V_{GNP} applied across the ET and ETDs.

Colour parameters

The colour parameters (K/S value, L^* , a^* , b^* , C^* , h^*) of the ETs and ETDs were acquired at various V_{GNP} using Xrite-8400 spectrophotometer under a D65 illumination using a 10° standard observer.

Conflicts of interest

There are no conflicts to declare.

Acknowledgements

The authors acknowledge funding from the National First-Class Discipline Program of Light Industry Technology and Engineering (LITE2018-21), the 111 Project (B17021), the National Natural Science Foundation of China (NO. 21975107), Fundamental Research Funds for the Central Universities (JUSRP51724B), the International Joint Research Laboratory for Advanced Functional Textile Materials, the China Scholarship Council (201706790076 and 201806790073), EPSRC grants EP/P02534X/2, EP/R511547/1, EP/T005106/1 and Trinity College, Cambridge. We wish to thank Dr Tian Carey and Mr Adrees Arbab for useful discussions.

References

- 1 J. Chen, Q. Peng, T. Thundat and H. Zeng, *Chem. Mater.*, 2019, **31**, 4553–4563.

- 2 Y. Guo, C. Dun, J. Xu, J. Mu, P. Li, L. Gu, C. Hou, C. A. Hewitt, Q. Zhang, Y. Li, D. L. Carroll and H. Wang, *Small*, 2017, 13, 1–9.
- 3 J. A. Rogers, T. Someya and Y. Huang, *Science* (80-), 2010, 327, 1603–1607.
- 4 R. Cao, X. Pu, X. Du, W. Yang, J. Wang, H. Guo, S. Zhao, Z. Yuan, C. Zhang, C. Li and Z. L. Wang, *ACS Nano*, 2018, 12, 5190–5196.
- 5 D. Na, J. Choi, J. Lee, J. W. Jeon and B. H. Kim, *ACS Appl. Mater. Interfaces*, 2019, 11, 27353–27357.
- 6 P. G. Karagiannidis, S. A. Hodge, L. Lombardi, F. Tomarchio, N. Decorde, S. Milana, I. Goykhman, Y. Su, S. V. Mesite, D. N. Johnstone, R. K. Leary, P. A. Midgley, N. M. Pugno, F. Torrissi and A. C. Ferrari, *ACS Nano*, 2017, 11, 2742–2755.
- 7 S. Yao, J. Yang, F. R. Poblete, X. Hu and Y. Zhu, *ACS Appl. Mater. Interfaces*, 2019, 11, 31028–31037.
- 8 C. Lv, L. Hu, Y. Yang, H. Li, C. Huang and X. Liu, *RSC Adv.*, 2015, 5, 25730–25737.
- 9 Y. Lu, X. Xiao, Z. Cao, Y. Zhan, H. Cheng and G. Xu, *Appl. Surf. Sci.*, 2017, 425, 233–240.
- 10 W. Zhang, X. Ji, C. Zeng, K. Chen, Y. Yin and C. Wang, *J. Mater. Chem. C*, 2017, 5, 8169–8178.
- 11 A. C. Siegel, S. T. Phillips, B. J. Wiley and G. M. Whitesides, *Lab Chip*, 2009, 9, 2775–2781.
- 12 Y. Li, Z. Zhang, X. Li, J. Zhang, H. Lou, X. Shi, X. Cheng and H. Peng, *J. Mater. Chem. C*, 2017, 5, 41–46.
- 13 I. J. Kim, M. Ramalingam and Y. A. Son, *Dye. Pigment.*, 2018, 151, 64–74.
- 14 M. Basson and T. S. Pottebaum, *Exp. Fluids*, 2012, 53, 803–814.
- 15 S. Hirata, K. S. Lee and T. Watanabe, *Adv. Funct. Mater.*, 2008, 18, 2869–2879.
- 16 L. S. Ribeiro, T. Pinto, A. Monteiro, O. S. G. P. Soares, C. Pereira, C. Freire and M. F. R. Pereira, *J. Mater. Sci.*, 2013, 48, 5085–5092.
- 17 C. Yu, Y. Zhang, D. Cheng, X. Li, Y. Huang and J. A. Rogers, *Small*, 2014, 10, 1266–1271.
- 18 A. Raditoiu, V. Raditoiu, C. A. Nicolae, M. F. Raduly, V. Amariutei and L. E. Wagner, *Dye. Pigment.*, 2016, 134, 69–76.
- 19 S. Ayazi-Yazdi, L. Karimi, M. Mirjalili and M. Karimnejad, *J. Text. Inst.*, 2017, 108, 856–863.
- 20 X. Geng, W. Li, Y. Wang, J. Lu, J. Wang, N. Wang, J. Li and X. Zhang, *Appl. Energy*, 2018, 217, 281–294.
- 21 F. Azizian, A. J. Field and B. M. Heron, *Dye. Pigment.*, 2013, 99, 431–439.
- 22 K. Ogasawara, K. Nakamura and N. Kobayashi, *J. Mater. Chem. C*, 2016, 4, 4805–4813.
- 23 X. Hu, X. Zhang, J. Liu and J. Dai, *Polym. Int.*, 2014, 63, 453–458.
- 24 X. Ji, W. Zhang, F. Ge, C. Wang, Y. Yin and K. Chen, *Prog. Org. Coatings*, 2019, 131, 111–118.
- 25 A. Bhattacharyya and M. Joshi, *Fibers Polym.*, 2011, 12, 734–740.
- 26 K. R. Karpagam, K. S. Saranya, J. Gopinathan and A. Bhattacharyya, *J. Text. Inst.*, 2017, 108, 1122–1127.
- 27 C. Wei, L. Fan, W. Rao, Z. Bai, W. Xu, H. Bao and J. Xu, *Cellulose*, 2017, 24, 5187–5196.
- 28 A. Laforgue, *J. Mater. Chem.*, 2010, 20, 8233–8235.
- 29 B. Zhou, Y. Li, G. Zheng, K. Dai, C. Liu, Y. Ma, J. Zhang, N. Wang, C. Shen and Z. Guo, *J. Mater. Chem. C*, 2018, 6, 8360–8371.
- 30 B. Zhou, M. Su, D. Yang, G. Han, Y. Feng, B. Wang, J. Ma, J. Ma, C. Liu and C. Shen, *ACS Appl. Mater. Interfaces*, , DOI:10.1021/acsami.0c09020.
- 31 B. Zhou, X. Han, L. Li, Y. Feng, T. Fang, G. Zheng, B. Wang, K. Dai, C. Liu and C. Shen, *Compos. Sci. Technol.*, 2019, 183, 107796.
- 32 A. Laforgue, S. Dubost, M. F. Champagne and L. Robitaille, *ACS Appl. Mater. Interfaces*, 2012, 4, 3136–3168.
- 33 H. Sun, D. Chen, C. Ye, X. Li, D. Dai, Q. Yuan, K. W. A. Chee, P. Zhao, N. Jiang and C. Te Lin, *Appl. Surf. Sci.*, 2018, 435, 809–814.
- 34 F. Torrissi, D. Popa, S. Milana, Z. Jiang, T. Hasan, E. Lidorikis and A. C. Ferrari, *Adv. Opt. Mater.*, 2016, 4, 1088–1097.
- 35 T. P. Call, T. Carey, P. Bombelli, D. J. Lea-Smith, P. Hooper, C. J. Howe and F. Torrissi, *J. Mater. Chem. A*, 2017, 5, 23872–23886.
- 36 J. Ren, C. Wang, X. Zhang, T. Carey, K. Chen, Y. Yin and F. Torrissi, *Carbon N. Y.*, 2017, 111, 622–630.
- 37 S. Qiang, T. Carey, A. Arbab, W. Song, C. Wang and F. Torrissi, *Nanoscale*, 2019, 11, 9912–9919.
- 38 T. Carey, S. Cacovich, G. Divitini, J. Ren, A. Mansouri, J. M. Kim, C. Wang, C. Ducati, R. Sordan and F. Torrissi, *Nat. Commun.*, 2017, 8, 1–11.
- 39 C. Celle, C. Mayousse, E. Moreau, H. Basti, A. Carella and J. P. Simonato, *Nano Res.*, 2012, 5, 427–433.
- 40 W. Lan, Y. Chen, Z. Yang, W. Han, J. Zhou, Y. Zhang, J. Wang, G. Tang, Y. Wei, W. Dou, Q. Su and E. Xie, *ACS Appl. Mater. Interfaces*, 2017, 9, 6644–6651.
- 41 Y. Yu, W. Shen, F. Li, X. Fang, H. Duan, F. Xu, Y. Xiong, W. Xu and W. Song, *RSC Adv.*, 2017, 7, 28670–28676.
- 42 G. Huang, L. Liu, R. Wang, J. Zhang, X. Sun and H. Peng, *J. Mater. Chem. C*, 2016, 4, 7589–7594.
- 43 D. Sui, Y. Huang, L. Huang, J. Liang, Y. Ma and Y. Chen, *Small*, 2011, 7, 3186–3192.
- 44 A. Abbas, Y. Zhao, J. Zhou, X. Wang and T. Lin, *Fibers Polym.*, 2013, 14, 1641–1649.
- 45 T. P. Call, T. Carey, P. Bombelli, D. J. Lea-Smith, P. Hooper, C. J. Howe, F. Torrissi, *J. Mater. Chem. A*, 2017, 23872 – 23886.
- 46 Z. Wang, Z. Ma, Y. Wang, Z. Xu, Y. Luo, Y. Wei and X. Jia, *Adv. Mater.*, 2015, 27, 6469–6474.